

# NUMERICAL SIMULATION OF COUPLED THERMO-HYDRO-MECHANICAL (THM) BEHAVIOR OF BUFFER MATERIAL IN THE CHINA-MOCK-UP TEST AT ENGINEERING SCALE

ZHAO Jingbo<sup>1</sup>, CAO Shengfei<sup>1</sup>, LI Jiebiao<sup>1, 2, 3</sup>, CHEN Liang<sup>1</sup>, COLLIN Frederic<sup>2</sup>, LIU Yuemiao<sup>1</sup>, ZHANG Qi<sup>1</sup>

<sup>1</sup> CAEA Innovation Center for Geological Disposal of High-Level Radioactive Waste, Beijing Research Institute of Uranium Geology, Beijing 100029, China;

<sup>2</sup> School of Environment, Harbin Institute of Technology, Harbin 150090, China;

<sup>3</sup> School of Environmental Science and Engineering, Southern University of Science and Technology, Shenzhen 518055, China;

<sup>4</sup> Departement GeomaC, University of Liege, Sart Tilman B52/3, Chevreuils Road, 1, B-4000 Liege, Belgium)

Corresponding author : E-mail: csf831016@163.com

## ABSTRACT

The buffer material plays a crucial role in the long-term safety of a high-level radioactive waste repository as it serves as a defense between the waste container and the host rock. To investigate the long-term performance of Gaomiaozi (GMZ) bentonite under repository conditions, based on the China-Mock-up test at engineering scale, the finite element code LAGAMINE is established to establish the THM numerical model. The complex boundary conditions and material properties involved in the test are considered, and the simulated results of temperature, relative humidity and swelling pressure are compared with the experimental ones over the past five years. The temperature in the China-Mock-up test is found to be periodic and linear, primarily influenced by the room temperature, which is accurately captured by the proposed model. Furthermore, the overall variation of the relative humidity at different locations is well reproduced. A desaturation-saturation process is observed in proximity to the heater, while it does not occur far from the heater. Additionally, the simulated results exhibit good agreement with the recorded data, effectively reflecting the increasing trend of stress over time. Besides, the interaction between temperature, humidity and stress of bentonite under the coupled THM conditions is achieved. These findings provide valuable insights into the long-term behavior of buffer materials in a repository environment and serve as an important reference for further understanding.

**KEY WORDS : BUFFER MATERIAL; CHINA-MOCK-UP TEST; COUPLED THM MODEL; GAOMIAOZI BENTONITE**

**CLC NUMBER : TU443 - DOCUMENT CODE : A - ARTICLE ID : 1000-4548(2024)08-1712-11**

## BIOGRAPHY

ZHAO Jingbo (1988-), male, Senior engineer, mainly engaged in the research of hydrogeology and buffer materials for geological disposal of high-level radioactive waste. E-mail: zhaojingbobiug@outlook.com

## FOUNDATION ITEM

The Project of Research on In-situ Testing and Installation Techniques for Buffer Materials in Beishan Underground Research Laboratory was funded by State Administration of Science, Technology and Industry for National Defense; National Natural Science Foundation of China (U2267217); Special Project for Decommissioning of Nuclear Facilities and Radioactive Waste Treatment (Grant Number :2022-736)

## 0. Introduction

The safe disposal of high-level radioactive waste (HLW) is a critical issue that relates to the sustainable development of nuclear industry, environmental protection, and public health. Currently, deep geological formations are internationally considered feasible method for the disposal of HLW, which are generally designed based on multiple barrier system concept<sup>[1]</sup>. As a crucial artificial barrier, buffer/backfill materials between the waste canister and the host rock will undergo complex coupled thermo-hydro-mechanical (THM) processes under the conditions of the radioactive decay heat, groundwater seepage and the surrounding rock stress. Consequently, evaluating the long-term performance is significant for the safety of HLW repositories<sup>[2]</sup>. Bentonite, such as MX-80, FEBEX, Kunigel V1 and Gaomiaozi bentonite, has been selected as buffer material for deep geological disposal of high-level radioactive waste in many countries due to its low permeability, excellent swelling capacity, water retention and long-term stability.

To investigate coupled THM behaviors of buffer materials under the conditions of HLW repositories, conducting model tests at an engineering scale is an essential approach. Nevertheless, due to the limitation of experimental time scale, it is necessary to carry out the corresponding numerical simulations to predict and evaluate the long-term performance of buffer materials. Therefore, the engineering-scale tests and numerical models are utilized to investigate the coupled THM properties of buffer materials in many underground research laboratories worldwide. Drawing on laboratory and in-situ experiments conducted at various scales in Swedish, different numerical models were developed to investigate the behaviors of temperature, hydraulic, and swelling pressure of MX-80 bentonite under repository conditions, utilizing different software/codes, including ABAQUS, CODE\_BRIGHT, and COMPASS<sup>[3-5]</sup>.

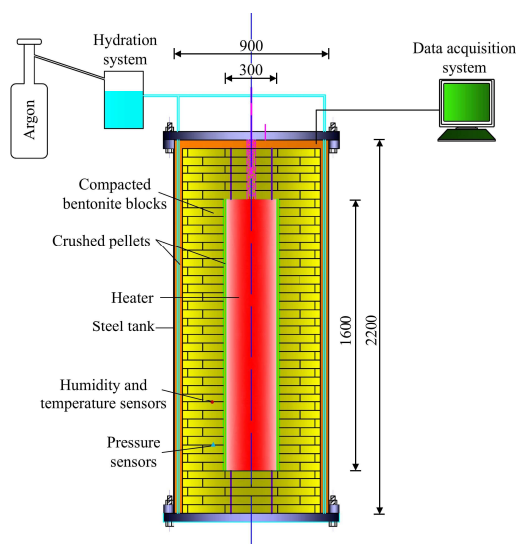
Meanwhile, a full-scale in-situ test (FE) and 1:2 scale heating test (HE-E) were also carried out at the Mont Terri underground research laboratory to investigate coupled THM responses of MX-80 bentonite in Switzerland, and the corresponding models were developed to reproduce the THM processes using the codes TOUGH 2 and OpenGeoSys<sup>[6-7]</sup>. Regarding FEBEX bentonite, similar studies were carried out through mock-up experiments in Madrid, Spain, and in-situ tests in Grimsel, Switzerland, with THM coupled mathematical and corresponding numerical models developed using different software<sup>[8-10]</sup>. At the AECL underground research laboratory in Canada, the mixture of bentonite and sand was selected as the buffer material, and the long-term evolution between the surrounding rock and the compacted buffer material was studied and simulated through the in-situ tests (BCE and ITT) and numerical methods at the engineering scale<sup>[11-13]</sup>. In addition, similar tests and numerical models have been conducted in other countries, including the KENTEX test in Korea, the Mock-Up-CZ test in the Czech Republic, and the OPHELIE Mock-Up test in Belgium<sup>[14-16]</sup>. Internationally, the DECOVALEX Project were established to advance the understanding and modeling of coupled thermo-hydro-mechanical-chemical (THMC) processes and to evaluate the feasibility of engineering barriers in geological systems. Furthermore, numerous constitutive models describing various mechanical behaviors of buffer materials, such as the BBM model and the BExM model, have been proposed<sup>[17-19]</sup>.

In China, Gaomiaozi (GMZ) bentonite from Inner Mongolia has been selected as the most suitable buffer material, and extensive experimental studies on its permeability, thermal conductivity, and mechanical properties have been conducted<sup>[20-22]</sup>. To investigate the long-term performance of GMZ bentonite under repository conditions, a mock-up facility, named the China-Mock-up, was installed in the Beijing Research Institute of Uranium Geology (BRIUG) and at engineering scale in 2011<sup>[23]</sup>. Chen et al.<sup>[24]</sup> and Zhao et al.<sup>[25]</sup> proposed the THM mathematical and numerical models of GMZ bentonite, and preliminarily validated the reliability of the corresponding models. In this paper, based on the previous research results, the finite element numerical code LAGAMINE was adopted to develop the coupled THM models, taking into account the complex boundary conditions and five different material properties. Additionally, the mathematical and numerical models of GMZ bentonite were further validated and well reproduced the coupled THM behaviors of the buffer material over the past five years. These findings provide crucial technical support for evaluating the long-term THM performance of buffer materials under repository conditions, significantly advancing our predictive capabilities for geological disposal systems.

## 1. China-Mock-up test

According to the conceptual model of HLW disposal in China, the China-Mock-up test is designed as a vertical cylinder. Its main components include a steel tank (inner diameter: 900 mm, height: 2200 mm, thickness: 25 mm), crushed pellets, compacted bentonite blocks, a heater (diameter: 300 mm, height: 1600 mm), a data acquisition system, a hydration system, a temperature control system, sensors, and other equipment, as shown in Fig. 1. The heater consists of a heater strip and a high thermal conductivity material. The gaps between the steel tank and the bentonite blocks, as well as between the heater and the bentonite blocks, are filled with crushed pellets (with thicknesses of 0.015 m and 0.05 m, respectively). The compacted bentonite primarily comprises fan-shaped blocks with a dry density of 1.71 g/cm<sup>3</sup>, an initial moisture content of 8.7%, and an initial suction of 80 MPa.

**Fig. 1.** Sketch of China-Mock-up test<sup>[23]</sup>



To systematically acquire data on temperature, humidity, swelling pressure, and deformation within the buffer material, ten different types of sensors, including temperature sensors, humidity sensors, stress sensors, displacement sensors, pore water pressure sensors, and resistance strain sensors, were installed. During installation process, particular emphasis was placed on the functional correlation and complementarity among sensors within each layer and between different layers. This system represents the largest coupled thermo-hydro-mechanical-chemical (THMC) test for buffer materials currently constructed in China and is capable of simulating the long-term coupled processes of buffer materials under repository conditions.

## 2. Coupled THM mathematical model

Chen et al.<sup>[24]</sup> proposed a mathematical model to describe the coupled THM behaviors of GMZ bentonite, aiming to better simulate the complex processes observed in the China-Mock-up test, such as heat transfer, liquid water migration, water vapor diffusion and condensation, and soil swelling and shrinkage. In this study, the same theoretical model is adopted, and a brief overview of the model is provided below.

### 2.1. WATER TRANSPORT EQUATION

There are two forms of water in bentonite: liquid water and water vapor. Each phase meets the conservation laws of mass, momentum, and energy. For the water, the mass conservation equation is derived by combining the balance equations of the liquid water and water vapor, which can be written as:

$$\underbrace{\frac{\partial(\rho_w n S_{r,w})}{\partial t} + \text{div}(\rho_w f_w)}_{\text{液态水}} + \underbrace{\frac{\partial(\rho_v n S_{r,g})}{\partial t} + \text{div}(i_v \rho_v f_g)}_{\text{水蒸气}} = 0 \circ (1)$$

(1)

Where  $\rho_w$  and  $\rho_v$  are the density of liquid water and water vapor;  $n$  is the porosity;  $t$  is the time;  $S_{r,w}$  and  $S_{r,g}$  are the saturation of water and water vapor;  $f_w$  and  $f_g$  are the velocities of water and water vapor;  $i_v$  is the dispersion of water vapor. To ensure good convergence and stability of the numerical model, it is assumed that gas pressure remains constant in the simulation process, and gas diffusion is ignored. Consequently, only the transport of liquid water in the porous medium is taken into consideration, which is governed by the generalized Darcy's law:

$$f_w = \frac{k_{int} k_{r,w}}{\mu} [\nabla p_w + \rho_w g \nabla y] \circ \quad (2)$$

Where  $p_w$  is the water pressure;  $k_{int}$  and  $k_{r,w}$  are the saturated permeability and relative permeability respectively;  $\mu$  is the dynamic viscosity coefficient.

## 2.2. HEAT TRANSPORT EQUATION

The thermal transport model is based on the conservation of energy law, assuming that all components of the material are in thermodynamic equilibrium and could be characterized using temperature. The governing equation incorporates the energy contributions of the solid, liquid, and gas phases, which could be expressed as:

$$\frac{\partial}{\partial t} [E_s \rho_s (1 - n) + E_w \rho_w S_{r,w} n + E_g \rho_g S_{r,g} n] + \nabla \cdot (i_c + j_{Es} + j_{Ew} + j_{Eg}) = Q \circ \quad (3)$$

Where  $E_s$ ,  $E_w$  and  $E_g$  represent the internal energy of solid, liquid and gas, respectively;  $i_c$  denotes the thermal conduction;  $j_{Es}$ ,  $j_{Ew}$  and  $j_{Eg}$  are the thermal convection in the solid, liquid and gas, respectively;  $Q$  is the source or sink term.

## 2.3. MECHANICAL CONSTITUTIVE MODEL

In this paper, the BBM model proposed by Alonso et al. [21] is used as the mechanical constitutive model, which can better reflect the significant impact of saturation on the mechanical properties of soil. Its LC yield surface can be described in the  $(p, q, s)$  three-dimensional space as:

$$q^2 - M^2(p + p_s)(p_0 - p) = 0 \circ \quad (4)$$

Where  $p$  is the mean stress;  $q$  is the deviatoric stress;  $M$  is the slope of the critical line;  $p_0$  is the pre-consolidation pressure;  $p_s$  is the soil strength in extension. There are LC yield line and SI yield line in  $(p, s)$  two-dimensional space, which could be expressed as, respectively:

$$\left. \begin{aligned} p_0 &= p_c \left( \frac{p_0^*}{p_c} \right)^{\frac{\lambda(0)-k}{\lambda(s)-k}}, \\ F_2 &= s - s_0 = 0 \circ \end{aligned} \right\} \quad (5)$$

Where  $p_0^*$  is the consolidation pressure in the saturated condition;  $p_c$  is the reference stress;  $s_0$  is the maximum suction at pre-consolidation;  $k$  is the elastic slope of the compressibility curve against the net mean stress;  $\lambda(0)$  and  $\lambda(s)$  is the compression parameter when the suction is  $s$  in the saturated state, and the relationship could be written as:

$$\lambda(s) = \lambda(0)[(1 - r) \exp(-\beta s) + r] \circ \quad (6)$$

Where  $r$  is the maximum stiffness parameter of the soil under the influence of suction;  $\beta$  is the parameter that controls the rate of increase in the stiffness coefficient of the soil with suction. The model hardening criterion could be expressed as:

$$\left. \begin{aligned} dp_0^* &= \frac{(1+n)1p_0^*}{\lambda(0)-k} d\varepsilon_v^p, \\ ds_0 &= \frac{(1+n)(s_0+p_{at})}{\lambda_s-k_s} d\varepsilon_v^p \circ \end{aligned} \right\} \quad (7)$$

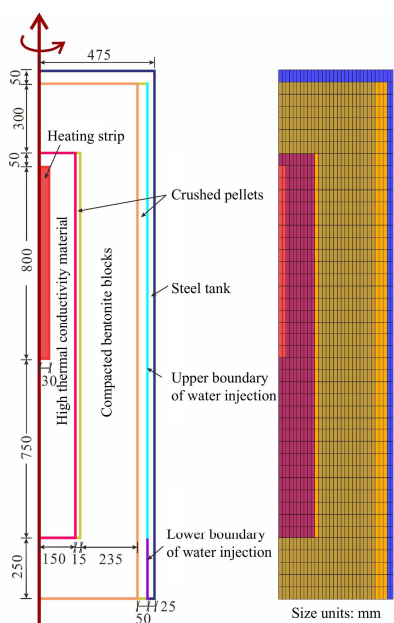
Where  $\lambda_s$  and  $k_s$  are the plastic stiffness parameter and the elastic stiffness parameter of the volume deformation caused by suction, respectively, and  $p_{at}$  is the standard atmospheric pressure.  $\varepsilon_v^p$  is the plastic volumetric strain.

### 3. Coupled THM numerical model

#### 3.1. MODEL STRUCTURE AND MESH DISCRETIZATION

Considering the actual structure of the China-Mock-up test, a 2D axisymmetric numerical model was established, incorporating five different materials namely, the heating strip, high thermal conductivity material, steel tank, compacted bentonite block, and crushed pellets. The results are shown in Figure 2. Each material is assumed to be homogeneous and isotropic, and the gaps between bentonite blocks and crushed pellets are ignored. Among them, the saturated permeability of crushed pellets is considered to be higher than that of compacted bentonite blocks, with values of  $2.5 \times 10^{-18}$  and  $2.5 \times 10^{-20} \text{ m}^2$ , respectively. Besides, the values of other parameters are assumed to be identical to those of compacted bentonite blocks. In this study, the finite element numerical code LAGAMINE developed by the University of Liège in Belgium, was employed. This code supports various types of mesh discretization and local refinement, and offers a series of constitutive models for describing the mechanical behavior of soils, such as the Mohr Coulomb model and the Barcelona Basic Model (BBM). It is capable of quantitatively simulating heat transfer, moisture migration, gas diffusion, and soil deformation under coupled multi-physical conditions. In the paper, rectangular grids with a total of 1482 elements and 4244 nodes were adopted (as illustrated in Fig. 2). Experimental data on temperature, relative humidity, and swelling pressure over a period of approximately five years were selected to validate the model.

**Fig. 2.** Numerical model for China-Mock-up test and mesh grids



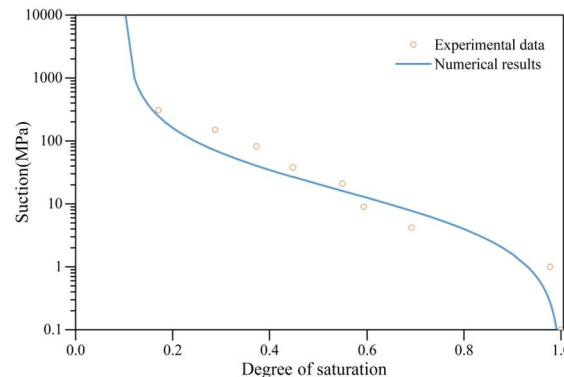
### 3.2. MODEL PARAMETER DETERMINATION

A series of experiments, including tests on soil-water characteristic curves, unsaturated permeability, compressibility, and thermal conductivity, were conducted in previous studies to provide the coupled THM parameters required for this study. For unsaturated soils, the relationship between suction ( $s$ ) and degree of saturation ( $S_{r,w}$ ) could be expressed as:

$$S_{r,w} = S_{r,res} + a_3 \frac{S_{r,u} - S_{r,res}}{a_3 + (a_1 s)^{a_2}} \quad (8)$$

In this equation,  $S_{r,u}$  represents the maximum degree of saturation, taken as 1.0, and  $S_{r,res}$  denotes the residual degree of saturation, assigned a value of 0.1. Based on the experimental soil-water characteristic data, the parameters in Eq. (8) were determined using the least squares method. The fitted results are presented in Fig. 3. The obtained parameters are:  $a_1 = 7.0 \times 10^{-6} \text{ Pa}^{-1}$ ,  $a_2 = 0.9$ , and  $a_3 = 70$ .

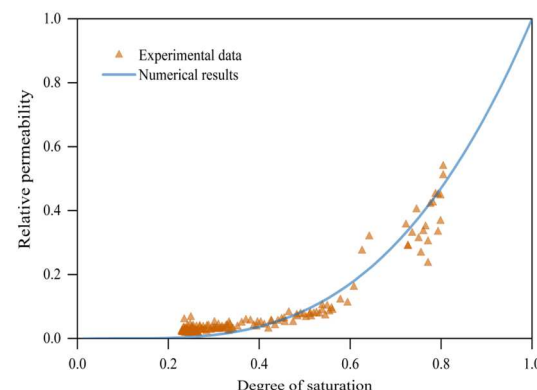
**Fig. 3.** Water retention curve of GMZ bentonite



In the unsaturated permeability tests, the instantaneous profile method was employed to determine the permeability coefficient of bentonite. The average permeability coefficient at a given section and time was calculated based on the measured flow rate and the hydraulic gradient. According to previously obtained experimental data, the fitted expression for the relative permeability  $k_{r,w}$  was given as (see Fig. 4):

$$k_{r,w} = \frac{(S_{r,w} - S_{r,res})^3}{(S_{r,u} - S_{r,res})^3} \quad (9)$$

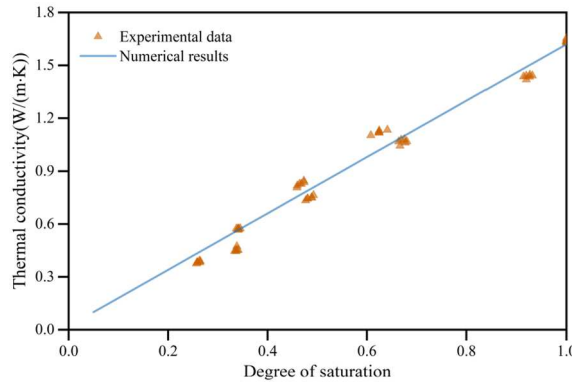
**Fig. 4.** Relative permeability of GMZ bentonite as a function of degree of saturation



Based on the thermal conductivity test, the relationship between the saturation degree  $S_{r,w}$  of GMZ bentonite and the thermal conductivity  $k$  was (Fig. 5)

$$k = 1.6S_{r,w} + 00.2 (R^2 = 0.976) \circ \quad (10)$$

**Fig. 5.** Thermal conductivity of GMZ bentonite as a function of degree of saturation



Since the currently available model parameters are relatively limited, the remaining parameters were adopted with reference to experimental data from representative bentonites studied abroad [24]

### 3.3. MODEL BOUNDARY CONDITIONS

During the test, the actual temperature boundary is divided into two parts: the heater strip and outer surface of China-Mock-up facility. The temperature of the heater strip was gradually increased according to the experimental design and eventually stabilized at 90 °C. During the first 255 days, the heating control system was relatively unstable, resulting in significant fluctuations in the measured data during the initial stage of the test. In the numerical model, the heating process was simplified as follows: the temperature was held constant at 30 °C from day 0 to day 135, then gradually increased from 30 °C to 90 °C between day 136 and day 255. After day 256, the temperature was maintained at 90 °C. Based on this, the heating process is simulated using the step function method, as shown in Fig. 6. Although thermal insulation material was installed on the outer surface of the facility, its effectiveness was relatively poor during the first 1,500 days of the test. As a result, the system was noticeably affected by room temperature and exhibited clear seasonal fluctuations. Subsequently, due to changes in the room environment, the temperature stabilized and fluctuated within a relatively narrow range. Based on this, the temperature boundary of outer surface in the numerical model is defined by segmentally fitting the experimental data using a combination of Fourier and linear functions. Notably, room temperature exhibits minor but distinct fluctuations around day 700. This behavior was addressed in the model through artificial boundary treatment, as illustrated in Fig. 7.

**Fig. 6.** Heating process and numerical results of heater strip

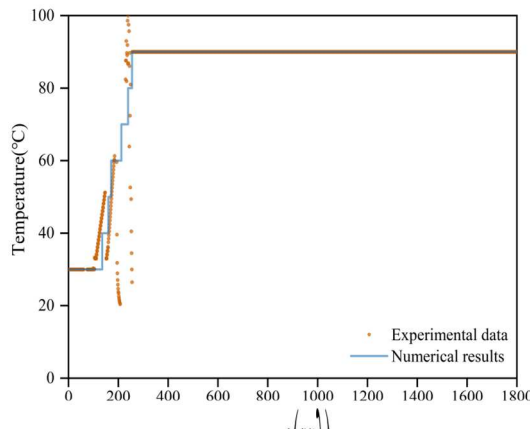
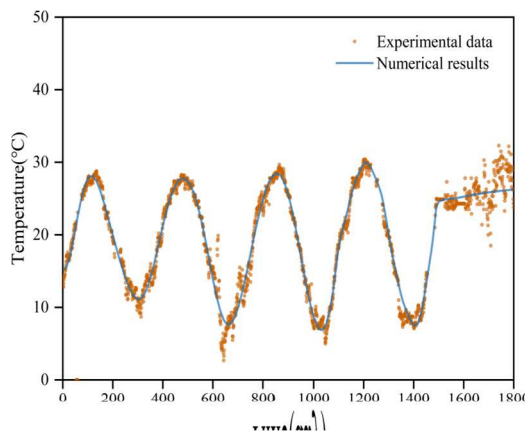
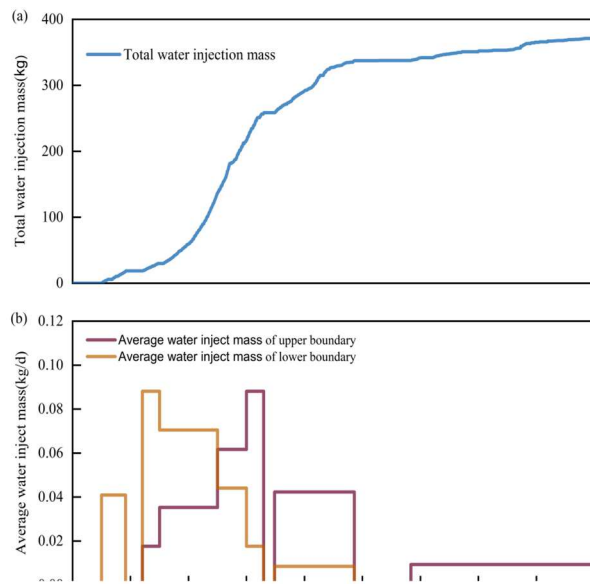


**Fig. 7.** Variation in room temperature and numerical results with time



The test water injection pipe is fixed on the inner wall of test cavity, with water injected from the bottom. The cumulative volume of injected water increased gradually over time, as shown in Fig. 8(a). During the actual injection process, due to the influence of gravity, more water accumulated in the lower part of the test facility compared to the upper area. To more accurately simulate the actual water injection conditions, the boundary in the model is divided into two sections, as shown in Fig. 2. In the early stage of the test, the amount of water injected into the upper part was relatively small, while the lower part received a larger volume. As the bentonite in the lower section gradually became saturated, the water injection volume in that area decreased over time, while the injection volume in the upper part increased accordingly. Considering the numerous test-related factors that influenced daily water injection volumes and the fact that the actual daily injection rates varied, a simplified approach was adopted in the numerical model. Average water injection rates were assigned to the upper and lower boundary sections to represent the overall water injection process, as illustrated in Fig. 8(b).

**Fig. 8.** Water injection process in China-Mock-up test



## 4. Results and discussion

### 4.1. THERMAL RESPONSE FIELD

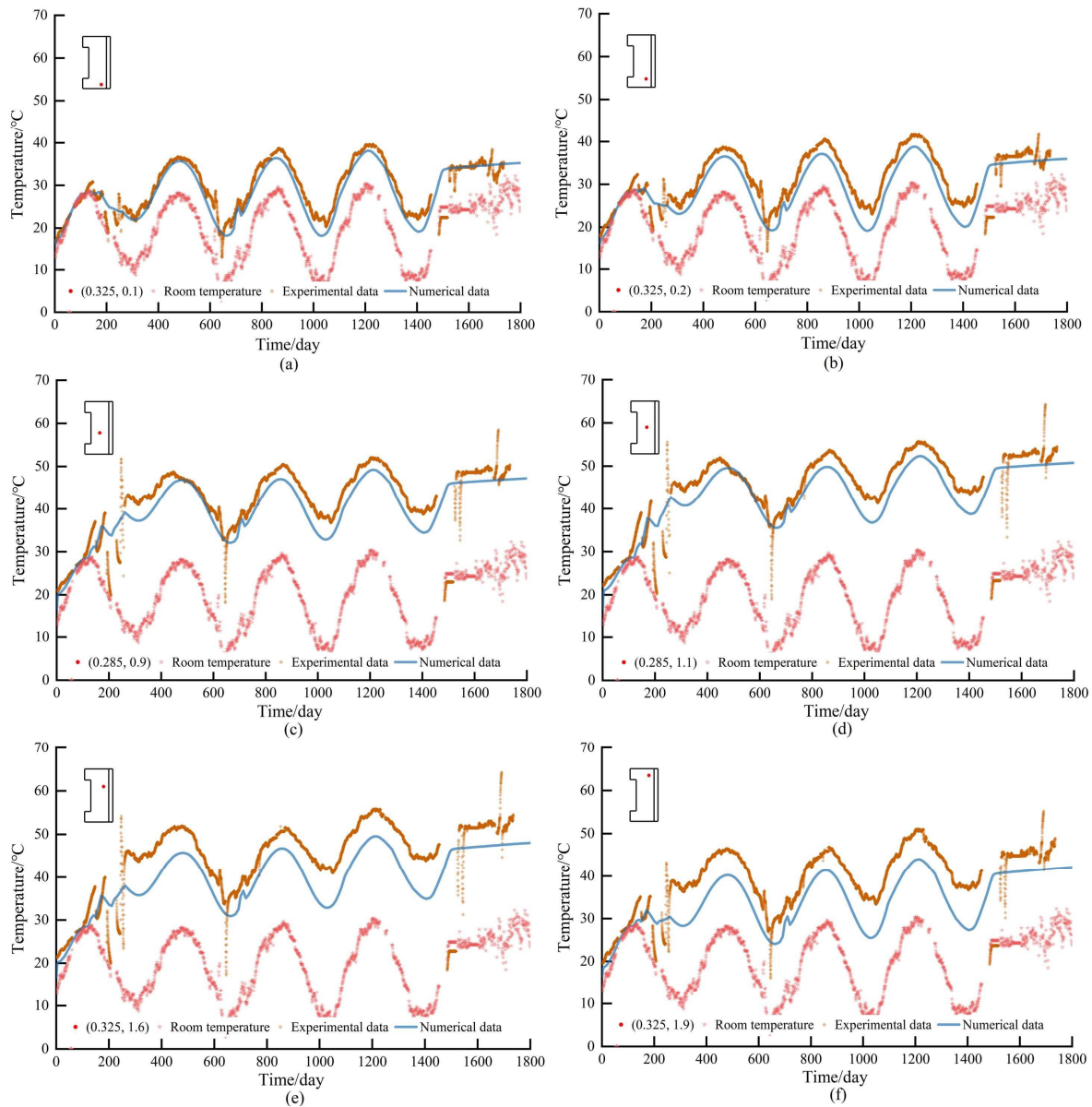
A comparison between the predicted and experimental data of the temperature at different locations is shown in Fig. 9. The results indicate that the numerical results are in good agreement with the experimental data, accurately reflecting the evolution of the temperature with time. This strongly demonstrates that the thermal parameters and boundary conditions set for each material in this study are reasonable. Furthermore, the temperature curves for different locations in Fig. 9 show significant fluctuations in response to changes in room temperature. In the numerical model, the external temperature boundary condition is defined using a piecewise function, which effectively captures the temperature fluctuation pattern during the early stage and its linear variation in the later stage. During the period from 0 to 255 days, the temperature at various locations is influenced by the combined effects of the heating strip and the room temperature. Specifically, between days 135 and 255, the boundary temperature of the heating strip increases stepwise, while the room temperature gradually decreases. The simulation results reflect the interplay between these two boundary conditions. The locations shown in Fig. 9(a) and (b) are relatively distant from the heating strip, and the corresponding simulation results are primarily influenced by the room temperature, exhibiting a decreasing trend. The locations shown in Fig. 9(c) ~ (f) are relatively close to the heating strip. During this period, the temperature of the heating strip increases from 80 °C to 90 °C, and the corresponding simulated temperatures exhibit a rising trend. Subsequently, as the system continues to evolve, the region influenced by the heating strip gradually reaches thermal equilibrium. Thereafter, room temperature becomes the dominant factor affecting the simulation results, leading to a gradual decline in the simulated temperatures. A similar

phenomenon is also observed around day 174. However, during this period, the overall temperature trend at the monitored locations is increasing, indicating that the heating strip continues to dominate the temperature evolution. Meanwhile, between 700 and 720 days, the observed temperature data exhibit slight fluctuations due to variations in room temperature, which are accurately captured by the proposed model. After 1500 days, room temperature fluctuations diminish, and the numerical model effectively simulates this behavior using a linear approximation.

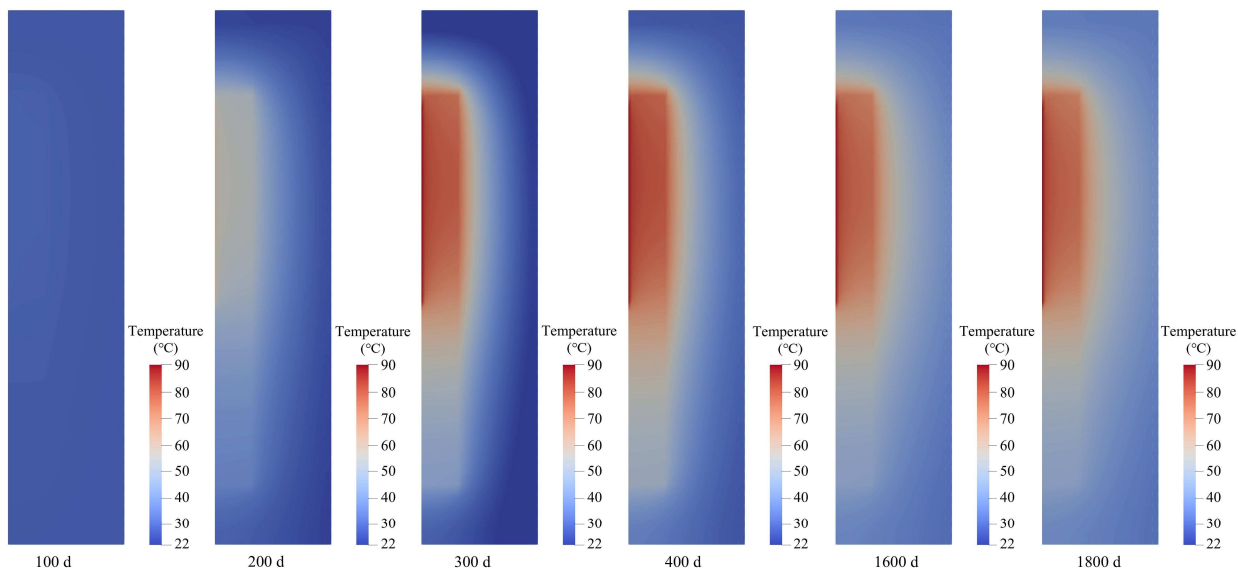
The simulation results in Fig. 9(e) and (f) also show that the numerical values at the upper locations are lower than the corresponding experimental data. This discrepancy is likely attributable to water evaporation caused by the operation of the heating strip, which generates water vapor as the temperature increases. The increased gas pressure in the higher temperature regions of the bentonite drives the vapor upward, transporting a portion of the heat with it and leading to higher measured temperatures in the upper regions compared to the numerical results. Due to the enclosed design of the test facility and the surrounding layer of thermal insulation, heat gradually accumulates in the upper area over time, causing a steady increase in temperature in that region. In the numerical simulation, to achieve better numerical convergence, it is assumed that the gas pressure within the bentonite remains constant over time, and the gas migration process is neglected. This simplification leads to simulated temperatures that are lower than the experimental measurements. Nevertheless, as shown in Fig. 9(a) and (b), the influence of this assumption is not significant at the bottom of the test facility.

Fig. 10 presents contour plots of the temperature field distribution of the test facility at different time. These results effectively reflect the differences in thermal conductivity among the various materials. As shown in Fig. 10, the highest simulated temperature occurs at the heating strip, high thermal conductivity material, which has good thermal conductivity, with only a slight temperature difference from the heating strip. In contrast, bentonite blocks and crushed pellets have relatively low thermal conductivity and are located near the outer boundary, making them more susceptible to the temperature. As a result, there is a more noticeable variation in temperature distribution across different locations within these materials. Furthermore, the simulation results indicate that at 100 days, the heating strip temperature remains at 30 °C, which is close to the room temperature, resulting in minimal temperature variation inside the test facility. As the temperature of the heating strip increases over time, the temperature of the high thermal conductivity material rises rapidly. By around 300 days, the temperature field reaches a relatively stable state, with fluctuations mainly driven by changes in room temperature. For example, at 300 days, the room temperature is approximately 8.7 °C, gradually increasing to 21.5 °C by 400 days. The temperature field contour plots effectively capture the temporal evolution of the temperature field within the test facility. A comparison of the temperature field contours at 1600 and 1800 days reveals that the room temperature fluctuates in an approximately linear pattern with only slight variation during this period. Consequently, the differences in the temperature field distribution are also minimal.

**Fig. 9** Comparison between predictive temperature and experimental results at different locations of China-Mock-up facility



**Fig. 10.** Temperature distribution at different time



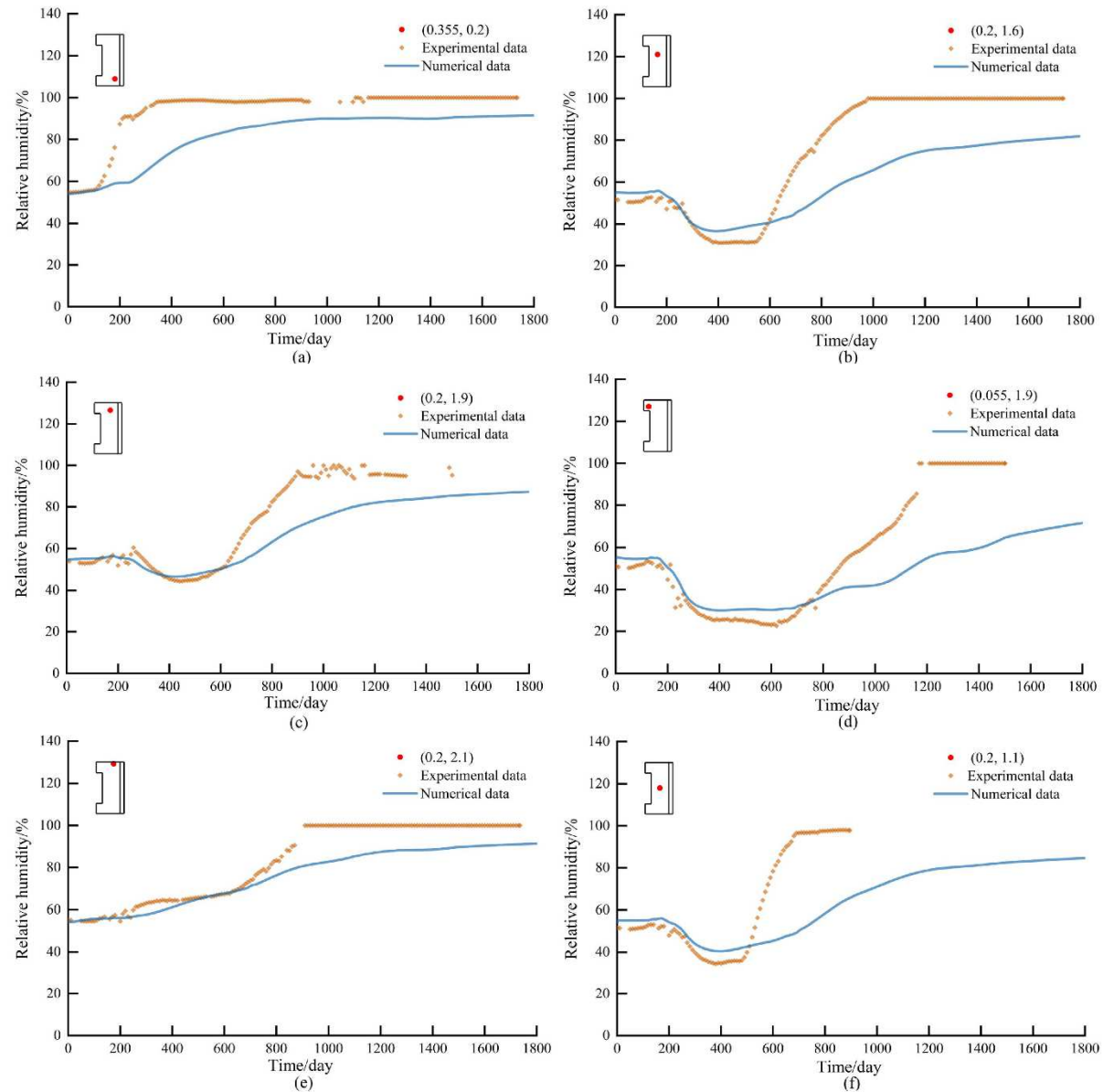
## 4.2. HYDRAULIC RESPONSE FIELD

Fig. 11 presents the simulation results of relative humidity at various locations within the test facility over time. Comparison between the numerical results and experimental data demonstrates that the simulation approach employed in this study effectively captures the moisture migration behavior in bentonite under coupled THM conditions. At the beginning, before heating and water injection started, the relative humidity remained stable over time. Once the heater started operating, a notable decrease in relative humidity was observed near the location adjacent to the heater strip, corresponding to the continued progression of the heating process. Due to the influence of water injection, the relative humidity gradually increases and approaches saturation, as shown in Fig. 11(b) ~ (d) and (f). During this stage, the relative humidity curve exhibits a trend of initial drying followed by saturation. However, the above phenomenon does not appear in Fig. 11 (a) and (e). The primary reason is that these two locations are close to the water injection boundary but relatively distant from the heating strip, making them predominantly influenced by the water injection process. Consequently, the relative humidity at two locations gradually increases over time. The simulation results presented in Fig. 11 demonstrate a good agreement with the experimental data during the early stages. For instance, within the first 600 days shown in Fig. 11(b) ~ (d), the simulation effectively captures the temporal variation of relative humidity during the test. However, as time progresses, the observed growth rate of relative humidity in the experiments significantly exceeds the numerical predicted results. This discrepancy arises because gaps exist between bentonite blocks, between the blocks and the sensors, and among the bentonite pellets. In the actual water injection process, water preferentially penetrates along these gaps and diffuses rapidly to the sensor locations. In contrast, the numerical simulation assumes a fully homogeneous and isotropic medium without these gaps. Moisture migration is modeled as a slow diffusion process governed by the permeability of these materials, which is considerably slower than the preferential flow along

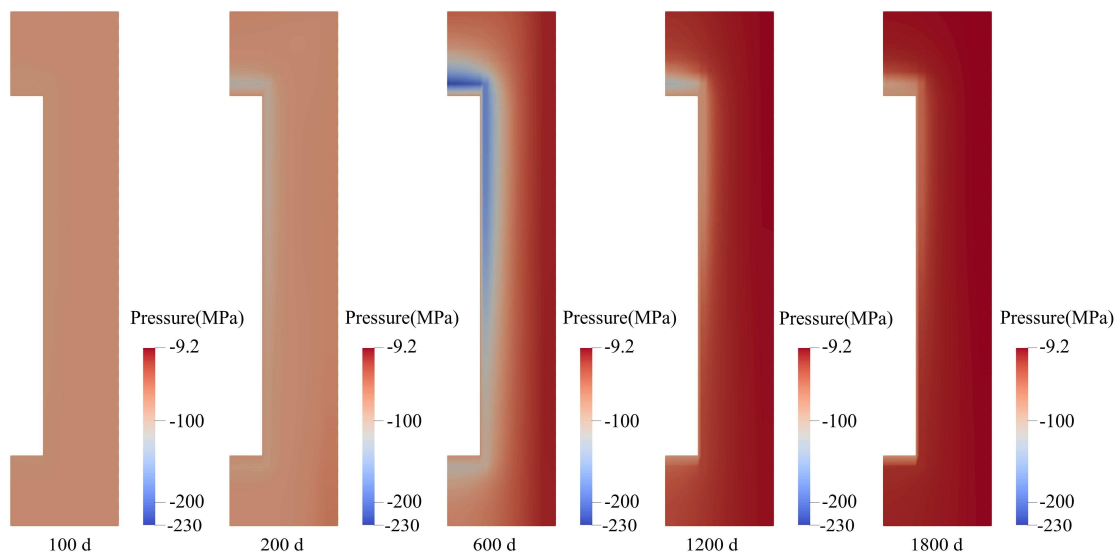
gaps. As a result, the simulation underestimates the relative humidity compared to the experimental data.

Fig. 12 shows the simulation results of the hydraulic response field during moisture migration within the bentonite at different times. During the first 100 days, the water pressure inside the bentonite remains consistent with the initial suction due to the temporary absence of water injection. Over time, the water pressure around the heater decreases as a result of the heating effect, reaching a minimum of approximately -230 MPa by 600 days. This simulation result aligns with the temporal variation in relative humidity shown in Fig. 11(b) ~ (d). Subsequently, with continued water injection, moisture gradually migrates from the outer regions toward the interior, causing the dry zone induced by heating to shrink and the water pressure within the soil to increase gradually. Additionally, the nephogram of the hydraulic response field indicates that after nearly five years of moisture migration, the bentonite in the test facility remains partially unsaturated, with a maximum water pressure of approximately -9.2 MPa. This clearly demonstrates the very low permeability of the bentonite blocks and the slow rate of moisture migration.

**Fig. 11.** Comparison between predictive relative humidity and experimental results at different locations of China-Mock-up facility



**Fig. 12.** Porewater pressure distribution at different times (Only the domains representing compacted bentonite blocks and crushed bentonite pellets are presented here)

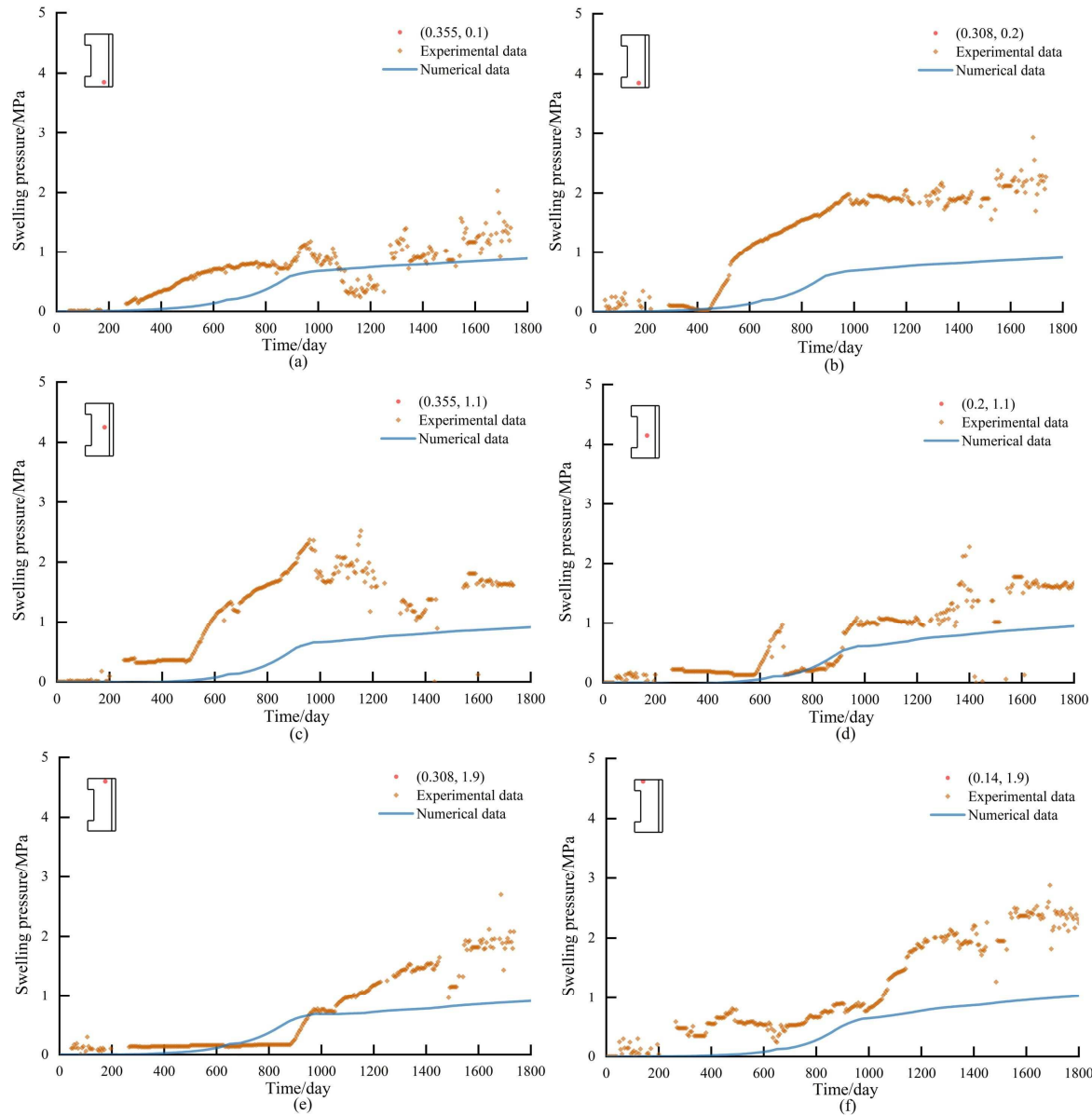


### 4.3. MECHANICAL RESPONSE FIELD

The evolution of swelling pressure in compacted bentonite blocks is a relatively complex process, primarily influenced by hydraulic and thermal effects. In this study, the swelling pressure is assumed to be uniform in all directions, and the anisotropic behavior of the material is not considered. Fig. 13 presents the variation of swelling pressure over time at different locations within the test facility. In this figure, the swelling pressure shown in Fig. 13(a) represents circumferential measurements, while the swelling pressure in Fig. 13(b) ~ (f) correspond to radial measurements. The simulation results indicate a gradual increase in swelling pressure over time, consistent with continued water injection. The model successfully reproduces the overall evolution of swelling pressure observed in the experimental data. In the central region, as shown in Fig. 13(d) and (e), swelling pressure at the two monitored locations increases slowly during the early stages of the test. This can be attributed to the combined effects of heating and the slow rate of moisture migration, given the extremely low permeability of bentonite. As suction gradually decreases, significant swelling is initiated. However, at some locations, the swelling pressure exhibits a pattern of initial decrease followed by two distinct increases during the test period, specifically between days 92 ~ 1176 and 1200 ~ 1500. This phenomenon can be explained by the existence of gaps between sensors and the compacted bentonite blocks, as well as between adjacent blocks. These gaps allow preferential moisture migration, leading to localized increases in swelling pressure. When water injection ceased, the resulting drop in water pressure caused a corresponding reduction in swelling pressure, as shown in Fig. 13(a) and (c). In the numerical model, it is currently challenging to accurately represent these gaps. Consequently, the simulated swelling pressure agrees reasonably well with experimental results during the initial stage of the test. However, as moisture begins to migrate rapidly along the actual gaps, the simulation underestimates the swelling pressure compared to the measured values. Despite these discrepancies, the model is still capable of capturing the overall swelling pressure

evolution of the bentonite blocks. This understanding provides a valuable reference for evaluating the long-term coupled performance of buffer materials under geological repository conditions.

**Fig. 13.** Comparison between predictive total stress and experimental results at different locations of China-Mock-up facility



## 5. Conclusions and recommendations

Considering five different material properties in the China-Mock-up test system, a coupled THM numerical model of GMZ bentonite under engineering scale conditions was established. This model can accurately simulate and predict the temperature evolution at various locations within the test facility over the past five years.

The simulation results show that, after nearly five years of operation, the bentonite in the test facility has not yet reached full saturation. The relative humidity at locations near the heater strip exhibits a trend of initial drying followed by gradual saturation, whereas at locations farther from the heater strip, the relative humidity increases over time. These results effectively capture the overall evolution of relative humidity behavior at different locations within the test facility.

There is a good agreement between the simulated swelling pressure and the experimental data, demonstrating that the model effectively captures the gradual increase in swelling pressure at different locations within the test facility over time. This understanding provides a valuable reference for evaluating the coupled THM performance of buffer materials under repository conditions.

To address the gaps between bentonite blocks and pellets, it is recommended that future laboratory tests be conducted to analyze the permeability and deformation behavior during the swelling process. Based on these findings, a constitutive model describing the gap-healing mechanism between bentonite blocks could be developed, along with a corresponding numerical simulation method for gap interfaces. Furthermore, considering the influence of host rock and groundwater at potential repository sites, it is suggested to carry out in-situ field experiments under coupled THM conditions at disposal depth. This would provide essential technical support for understanding the behavioral evolution of buffer materials in a real repository environment.

## References

1. GUO Yonghai, WANG Ju, JIN Yuanxin. The general situation of geological disposal repository siting in the world and research progress in China[J]. *Earth Science Frontiers*, 2001, 8(2): 327-332. (in Chinese)
2. CAO Shengfei, LIU Yuemiao, XIE Jingli, et al. Study on thermo-hydro-mechanical coupling behaviors of buffer material[J]. *Chinese Journal of Underground Space and Engineering*, 2020, 16(4):1123-1129. (in Chinese)
3. CLEALL P J, MELHUIS T A, THOMAS H R. Modelling the three-dimensional behaviour of a prototype nuclear waste repository[J]. *Engineering Geology*, 2006, 85(1/2): 212-220.
4. HÖEKMARK H, LEDESMA A, LASSABATERE T, et al. Modelling heat and moisture transport in the ANDRA/SKB temperature buffer test[J]. *Physics and Chemistry of the Earth*, 2007, 32(8-14): 753-766.
5. BAG R. Coupled Thermos-Hydro-Mechanical-Chemical Behaviour of MX80 Bentonite in Geotechnical Applications[D]. Cardiff: Cardiff University, 2011.
6. MÜELLER H R, WEBER H P, KÖEHLER S, et al. The full-scale Emplacement (FE) Experiment at the Mont Terri URL[C]// 5th International Conference on Clays in Natural & Engineered Barriers for Radioactive Waste Confinement, Montpellier, 2012.
7. WANG X R, SHAO H, WANG W Q, et al. Numerical modeling of heating and hydration experiments on bentonite pellets[J]. *Engineering Geology*, 2015, 198: 94-106.
8. SAMPER J, ZHENG L, MONTENEGRO L, et al. Coupled thermo-hydro-chemical models of compacted bentonite after FEBEX in situ test[J]. *Applied Geochemistry*, 2008, 23(5): 1186-1201.
9. MICHALEC Z, BLAHETA R, HASAL M, et al. Fully coupled thermo-hydro-mechanical model with oversaturation and its validation to experimental data from FEBEX experiment[J]. *International Journal of Rock Mechanics and Mining Sciences*, 2021, 139: 104567.
10. XU H, ZHENG L, RUTQVIST J, et al. Numerical study of the chemo-mechanical behavior of FEBEX bentonite in nuclear waste disposal based on the Barcelona expansive model[J]. *Computers and Geotechnics*, 2021, 132: 103968.
11. THOMAS H R, CLEALL P J, DIXON D, et al. The coupled thermal-hydraulic-mechanical behaviour of a large-scale in situ heating experiment[J]. *Géotechnique*, 2009, 59 (4): 401-413.
12. GUO R P, DIXON D, CHANDLER N. Use of numerical simulations to assess hydraulic and mechanical measurements of bentonite-sand buffer in an in-floor borehole[J]. *Engineering Geology*, 2010, 114(3/4): 433-443.
13. GUO R P. Thermo-hydro-mechanical modelling of the buffer/container experiment[J]. *Engineering Geology*, 2011, 122(3): 303-315.
14. CHO W J, LEE J O, KWON S. Analysis of thermo-hydro-mechanical process in the engineered barrier system of a high-level waste repository[J]. *Nuclear Engineering and Design*, 2010, 240(6): 1688-1698.

15. PACOVSKÝ J, SVOBODA J, ZAPLETAL L. Saturation development in the bentonite barrier of the Mock-Up-CZ geotechnical experiment[J]. Physics and Chemistry of the Earth, 2007, 32(8/9/10/11/12/13/14): 767-779.
16. ROMERO E, LI X L. Thermo-hydro-mechanical characterization of OPHELIE backfill mixture[J]. Chinese Journal of Rock Mechanics and Engineering, 2006, 25(4): 733-740.
17. RUTQVIST J, BARR D, BIRKHOLZER J T, et al. Results from an international simulation study on coupled thermal, hydrological, and mechanical processes near geological nuclear waste repositories[J]. Nuclear Technology, 2008, 163(1): 101-109.
18. ALONSO E E, GENS A, JOSA A. A constitutive model for partially saturated soils[J]. Géotechnique, 1990, 40(3): 405-430.
19. ALONSO E E, VAUNAT J, GENS A. Modelling the mechanical behaviour of expansive clays[J]. Engineering Geology, 1999, 54(1/2): 173-183.
20. WANG Ju, CHEN Weiming, SU Rui, et al. Geological disposal of high-level radioactive waste and its key scientific issues[J]. Chinese Journal of Rock Mechanics and Engineering, 2006, 25(4): 801-812. (in Chinese)
21. CUI Y J, TANG A M, QIAN L X, et al. Thermal-mechanical behavior of compacted GMZ bentonite[J]. Soils & Foundations, 2011, 51(6): 1065-1074.
22. YE W M, WAN M, CHEN B, et al. An unsaturated hydraulic conductivity model for compacted GMZ01 bentonite with consideration of temperature[J]. Environmental Earth Sciences, 2014, 71(4): 1937-1944.
23. CHEN L, LIU Y M, WANG J, et al. Investigation of the thermal-hydro-mechanical (THM) behavior of GMZ bentonite in the China-Mock-up test[J]. Engineering Geology, 2014, 172(8): 57-68.
24. CHEN L, WANG J, LIU Y M, et al. Numerical thermo-hydro- mechanical modeling of compacted bentonite in China-mock- up test for deep geological disposal[J]. Journal of Rock Mechanics and Geotechnical Engineering, 2012, 4(2): 183-192.
25. ZHAO J B, CHEN L, COLLIN F, et al. Numerical modeling of coupled thermal-hydro-mechanical behavior of GMZ bentonite in the China-Mock-up test[J]. Engineering Geology, 2016, 214: 116-126.